# Catalytic Mechanism of Golgi-Resident Human Tyrosylprotein Sulfotransferase-2: A Mass Spectrometry Approach

Lieza M. Danan,[a] Zhihao Yu,[a] Peter J. Ludden,[a] Weitao Jia,[a] Kevin L. Moore,[b,c,d] and Julie A. Leary[a]

[a] Department of Molecular and Cellular Biology, University of California, Davis, California, USA
[b] Cardiovascular Biology Research Program, Oklahoma Medical Research Foundation, Oklahoma City, Oklahoma, USA
[c] Departments of Cell Biology and Medicine, University of Oklahoma Health Sciences Center, Oklahoma City, Oklahoma, USA
[d] Oklahoma Center for Medical Glycobiology, University of Oklahoma Health Sciences Center, Oklahoma City, Oklahoma, USA

Human tyrosylprotein sulfotransferases catalyze the transfer of a sulfuryl moiety from the universal sulfate donor PAPS to the hydroxyl substituent of tyrosine residues in proteins and peptides to yield tyrosine sulfated products and PAP. Tyrosine sulfation occurs in the trans-Golgi network, affecting an estimated 1% of the tyrosine residues in all secreted and membrane-bound proteins in higher order eukaryotes. In this study, an effective LC-MS-based TPST kinetics assay was developed and utilized to measure the kinetic properties of human TPST-2 and investigate its catalytic mechanism when G protein-coupled CC-chemokine receptor 8 (CCR8) peptides were used as acceptor substrates. Through initial rate kinetics, product inhibition studies, and radioactive-labeling experiments, our data strongly suggest a two-site ping-pong model for TPST-2 action. In this mechanistic model, the enzyme allows independent binding of substrates to two distinct sites, and involves the formation of a sulfated enzyme covalent intermediate. Some insights on the important amino acid residues at the catalytic site of TPST-2 and its covalent intermediate are also presented. To our knowledge, this is the first detailed study of the reaction kinetics and mechanism reported for human TPST-2 or any other Golgi-resident sulfotransferase. (J Am Soc Mass Spectrom 2010, 21, 1633–1642) © 2010 Published by Elsevier Inc. on behalf of American Society for Mass Spectrometry

Sulfotransferases (ST) catalyze the transfer of a sulfuryl group ($SO_3$) from a donor molecule, usually 3′-phosphoadenosine 5′-phosphosulfate (PAPS), to a variety of amine- and hydroxyl-containing substrates, including proteins [1, 2], carbohydrates [3, 4] and low molecular weight metabolites [5, 6], as nucleophiles. There are two classes of STs: cytosolic STs, which are involved in detoxification, hormone regulation, and drug metabolism, and membrane-associated STs, which were identified recently as central players in a number of molecular recognition events and biochemical signaling pathways [7]. Moreover, sulfotransferases play a significant role in modulating normal and pathophysiologic processes [3, 8].

Because of STs biological importance and medical relevance, there is an intense interest towards understanding the exact functions of these enzymes. Early studies focused on cytosolic STs structure, substrate specificity, and kinetic mechanism through crystallographic and mutational studies which provided critical information about the active site residues involved in substrate binding and ST catalysis [7]. Direct kinetic analyses were performed as well to investigate the catalytic mechanism of several cytosolic and bacterial sulfotransferases. Initial rate studies have described distinct modes of catalysis for different STs including: (1) ordered Bi Bi mechanism was elucidated for phenol (SULT1A1 and SULT1A3) [9, 10] and flavonol (SULT201A1) [11] sulfotransferases; (2) random Bi Bi mechanism for estrogen sulfotransferase (SULT1E1) [12], retinol dehydratase [13], and Stf0 sulfotransferase [14]; and, (3) ping pong mechanism was reported for bacterial arylsulfate (ASST) [15] and NodH sulfotransferase (NodST) [16, 17].

A strong interest on the molecular enzymology of membrane-associated STs, such as tyrosylprotein sulfotransferases (TPSTs) and carbohydrate STs, evolved when studies showed that sulfation of cell-surface proteins by these enzymes appear to trigger vital molecular-recognition and signal-transduction events [2, 3]. For example, tyrosine sulfation of G protein-coupled chemokine receptors CCR8, CCR5, CCR2, CX3CR1, CXCR4, and

Address reprint requests to Dr. J. A. Leary, Department of Molecular and Cellular Biology, University of California, One Shields Ave., Davis, CA 95616, USA. E-mail: jaleary@ucdavis.edu


1044-0305/10/$32.00
doi:10.1016/j.jasms.2010.03.037

Published online April 2, 2010
Received November 2, 2009
Revised March 8, 2010
Accepted March 12, 2010

CXCR3 promote optimal binding with their respective chemokines [1, 18–23]. Interaction between the receptors and their ligands direct the migration of leukocytes for homeostatic purposes and in response to pro-inflammatory signals. Despite this biological significance, structural and mechanistic information on these Golgi-resident sulfotransferases are limited [24–27].

Two tyrosylprotein sulfotransferase isozymes have been identified, TPST-1 and TPST-2 (EC 2.8.2.20). These STs catalyze sulfuryl group transfer from PAPS to tyrosine residues within highly acidic motifs in proteins and peptides [28–30]. Human TPST-1 and -2 are ~50 kDa type-II transmembrane glycoproteins located in the trans-Golgi network. They share ~65% sequence homology and both are composed of a short N-terminal cytoplasmic domain, a single 17-residue transmembrane domain, and a luminal catalytic domain [31]. Both TPST-1 and -2 are broadly co-expressed in mammalian cells [28–30, 32, 33]. It was estimated that up to 1% of all tyrosine residues in the eukaryotic proteome are sulfated making it a very widespread post-translational modification [32–34].

In-depth characterization of TPST isozymes has been hampered by two factors; the lack of homogenous enzyme preparations, and a fast and accurate assay for quantitative kinetics analysis. Most previous reports on kinetic properties of TPST have employed crude enzymes [35–37] or highly enriched TPST from adrenal medulla [38] without knowing if both isozymes are present or not. In most of these studies, radioactive labeling assays using [$^{35}$S]PAPS were used to monitor the formation of sulfated products. Accuracy of these methods can vary greatly, thus compromising the correctness of the kinetic parameters reported. More importantly, these methodologies only allow the monitoring and quantification of total sulfation of tyrosine residues in products and could not differentiate between mono-, di-, and trisulfated products, which are present in many natural substrates such as CCR8 and CCR5. Recently, we developed a new LC-MS-based enzyme assay to monitor the formation of the mono- and disulfated products of CCR8 using reverse-phase (RP) HPLC coupled directly to a linear ion trap mass spectrometer equipped with an electrospray ionization source (ESI-MS) [39]. Using this method, the apparent kinetic parameters were obtained for purified recombinant human TPST-1 and TPST-2.

In this study, we present a detailed mechanistic characterization of recombinant human TPST-2-catalyzed sulfuryl group transfer from PAPS to two different acceptor peptides modeled on the N-terminus of human CCR8 (Figure 1) using our LC-MS-based assay. We chose to work with TPST-2 since our previous research showed that it's turnover number is ten times higher than TPST-1, although studies are ongoing to gain mechanistic insight into TPST-1 as well [39]. The catalytic mechanism of TPST-2 was determined to be a rapid equilibrium random two-site ping pong mechanism by initial rate kinetics and product inhibition studies, and confirmed by detection of a sulfated-enzyme covalent intermediate. Some insights on the TPST-2 active site and covalent intermediate are also presented based on chemical modification experiments and multiple sequence alignment with different STs. These are the first data reported on the reaction mechanism of human TPST-2, a Golgi-resident sulfotransferase.

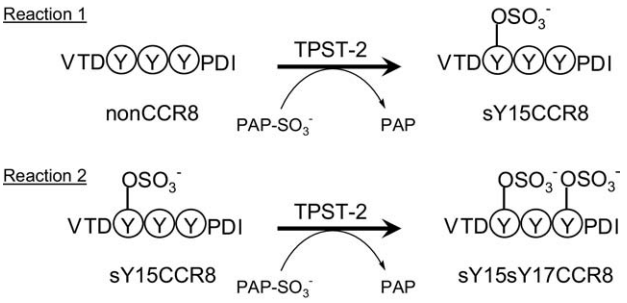


**Figure 1.** Tyrosine sulfation of CCR8 peptides by TPST-2. Reaction 1 shows the sulfation of nonsulfated CCR8 to monosulfated product sY15CCR8 while reaction 2 shows the formation of the disulfated product sY15sY17CCR8 from monosulfated sY15CCR8.

## Experimental

### *Materials*

Human CCR8 peptides (amino acids 12–20), VTDYYYPDI (nonCCR8), VTD**s**YYYPDI (sY15CCR8), VTD**s**YY**s**YPDI (sY15sY17CCR8), and the sY15CCR8 I20G variant (VTD**s**YYYPDG) were synthesized and HPLC-purified to ≥95% purity by Quality Controlled Biochemicals (QCB, Hopkinton, MA, USA). PAPS (≥95% purity) was prepared in-house as described previously [40]. All reagents used were of analytical grade and were purchased from Sigma-Aldrich (St. Louis, MO, USA), while HPLC-grade solvents were from Fisher Scientific (Fairborn, NJ, USA). Peptide concentrations were determined using UV-Vis spectroscopy at 280 nm with $\in_{280}$ = 3840 $cm^{-1}$ $M^{-1}$ at pH 7.0 for nonCCR8, and at 260 nm $\in_{260}$ = 283 $cm^{-1}$ $M^{-1}$ for sY15CCR8, sY15sY17CCR8, and the sY15CCR8 I20G variant.

### *TPST-2 Assay*

A recombinant epitope-tagged soluble form of human TPST-2 was used in all studies. In the recombinant enzyme, the native N-terminal 24 amino acids of TPST-2, including the cytoplasmic and transmembrane domain were replaced with the transferrin signal peptide (MRLAVGALLVCAVLGLCLA) followed by the 12-residue epitope for the $Ca^{+2}$-dependent mAb HPC4 [28]. Thus, the N-terminus of the recombinant soluble enzyme is $NH_2$-EDQVDPRLIDGKDPG$^{25}$Q (HPC4 epitope is underlined) after signal peptide cleavage. The recombinant soluble enzyme was purified from permanently-transfected CHO-K1 cells by HPC4 affinity chro-

matography. The recombinant enzyme is secreted as a disulfide-linked dimer and was assayed as previously reported [39]. Briefly, TPST-2 was assayed in the forward direction by monitoring the formation of the sulfated products of the two reactions in Figure 1. One unit (U) is equal to 1 μmol product formed per min.

All reaction mixtures contained 20 mM 3-(N-morpholino) propanesulfonic acid (MOPS), pH 7.5, 100 mM NaCl, and 10% (wt/vol) glycerol in addition to substrates, inhibitors, and enzymes, in a final volume of 60 μL, and were incubated at 30 °C. Reaction time optimization for Reaction 2 was performed on 1 μM TPST-2 allowing it to proceed from 3 to 110 min (Supporting Information 1, which can be found in the electronic version of this article). Optimal reaction time with linear response of substrate to product conversion can be reached when $T_q$ is ≤20 min (Supporting Information 1, insert). A similar optimization experiment for Reaction 1 was performed and published previously [39]. All reactions were initiated by the addition of 250–750 nM TPST-2 with a total reaction time varied from 6 to 20 min and were quenched by the addition of methanol containing 0.5 μM final concentration of the internal standard (IS), VTDsYYYPDG peptide. This peptide was chosen as the IS since its molecular mass and ionization efficiency are very similar to the sulfated products. Under these conditions, all initial velocity reactions converted less than 10% of the substrates to products. In most cases, no more than 5% of substrates were utilized at the end of the reaction. The product concentrations were very low therefore product inhibitions were negligible. Before sample introduction into the LC-MS system, quenched reaction mixtures were diluted with 20 mM ammonium acetate.

## Mass Spectrometry

All mass spectra were acquired on an LTQ linear ion trap mass spectrometer with a Surveyor HPLC system coupled to an electrospray ionization source (Thermo Electron, San Jose, CA, USA). Analytical samples were separated on a Zorbax Eclipse XDB C8 column (3 μm, 80 Å) (Agilent Technologies, Palo Alto, CA, USA) using a gradient from 2 to 100% eluent B over 30 min at a flow rate of 75 μL/min (eluent A, 20 mM ammonium acetate, pH 7, in water; eluent B, 20 mM ammonium acetate, pH 7, in 80% acetonitrile). The first 5 min of the analytical run was directed to waste for desalting purposes and then redirected to the ion source for MS analysis in the negative ionization mode. The ion transfer capillary was heated to 225 °C and the spray voltage was held at a potential of 3.5 kV. Selected ion monitoring (SIM) mode was used for quantification, focusing on the total ion count (TIC) peak areas representing the IS and the product. Twenty scans for each of the IS and product chromatographic peaks were averaged and used to determine their peak intensity ratio ($I_P/I_{IS}$). This ratio is directly related to product concentration and was used to determine the unknown concentrations of subsequent products formed.

## Quantification

For quantification purposes, both the singly-charged and the doubly-charged species of each peptide were monitored in SIM and their intensities, $I$, were summed to obtain their respective total intensities, $I_{TOT}$.

$$\mathrm{I_{TOT}\ (peptide)} = \mathrm{I_{(singly\text{-}charged)}} + \mathrm{I_{(doubly\text{-}charged)}} \quad (1)$$

A seven-point calibration curve was used for product quantification where the samples contained varying concentrations of the monitored product while keeping the IS concentration constant. Each of the calibration standards was analyzed in SIM mode to obtain the ratio of the intensity of the product ($I_P$) and the IS ($I_{IS}$), $I_P/I_{IS}$. Calibration curves were generated from $I_P/I_{IS}$ versus [product]/[IS] plots and the slope of the line, m, was calculated such that [P] from each subsequent reaction could be determined from eq 2.

$$[\mathrm{Product}] = (I_P/I_{IS}) \times [\mathrm{IS}]/\mathrm{m} \quad (2)$$

Once [P] is calculated, it can be used to calculate the velocity of the reaction, $\upsilon$, at any given substrate concentration and quench time, $T_q$, of the reaction by using eq 3:

$$\upsilon = [\mathrm{P}]/\mathrm{T_q} \quad (3)$$

## Data Analysis

Initial velocity data were first analyzed graphically using primary plots of $1/\upsilon$ versus $1/[S]$ using DeltaGraph Pro 4.05c, where [S] equals substrate concentration. Slopes and intercepts obtained from the primary plots were then graphed as secondary plots against the reciprocal concentrations of the fixed substrates and product inhibitor concentrations. The form of the overall rate equation was determined by examination of the results of graphical analysis. Final values for kinetic constants shown in Table 1 were obtained by fitting all data used in primary plots to the overall rate equation. Data were then each fitted for: (1) the ping-pong initial velocity pattern to eq 4, (2) competitive inhibition to eq 5, and (3) noncompetitive inhibition to eq 6 [41].

$$\upsilon = V_{max}\,[\mathrm{A}]\,[\mathrm{B}]/(K_{mB}[\mathrm{A}] + K_{mA}[\mathrm{B}] + [\mathrm{A}]\,[\mathrm{B}]) \quad (4)$$

$$\upsilon = V_{max}\,[\mathrm{A}]/\left\{K_{mA}\,(1 + [\mathrm{I}]/K_I) + [\mathrm{A}]\right\} \quad (5)$$

$$\upsilon = V_{max}\,[\mathrm{B}]/\left\{K_{mB}\,(1 + [\mathrm{I}]/K_I) + [\mathrm{B}]\,(1 + [\mathrm{I}]/K_I)\right\} \quad (6)$$

In these equations, $\upsilon$ represents the measured velocity, $V_{max}$ is the maximum velocity, A and B are substrates,

**Table 1.** Kinetic constants of human TPST-2[a] at 30°C

| Constant | Description | Mean ± SD | Units |
|---|---|---|---|
| Reaction 1: sulfation of nonCCR8 | | | |
| $V_{max}$ | Maximal velocity of sulfation of nonCCR8 | 7.1 ± 0.2 | mU/mg protein |
| $K_{mA}$ | Michaelis constant for nonCCR8 peptide at saturating PAPS | 19.3 ± 1.8 | μM |
| $K_{mB}$ | Michaelis constant for PAPS at saturating nonCCR8 peptide | 8.7 ± 0.3 | μM |
| $K_I$ | Product inhibition constant for PAP versus PAPS | 0.74 | μM |
| $K_I'$ | Product inhibition constant for PAP versus nonCCR8 | 1.2 | μM |
| Reaction 2: sulfation of sY15CCR8 | | | |
| $V_{max}$ | Maximal velocity of sulfation of sY15CCR8 | 1.8 ± 0.1 | mU/mg protein |
| $K_{mA}$ | Michaelis constant for sY15CCR8 peptide at saturating PAPS | 3.1 ± 0.2 | μM |
| $K_{mB}$ | Michaelis constant for PAPS at saturating nonCCR8 peptide | 4.8 ± 0.8 | μM |
| $K_I$ | Product inhibition constant for PAP versus PAPS | 0.16 | μM |
| $K_I'$ | Product inhibition constant for PAP versus sY15CCR8 | 3.8 | μM |

[a]The kinetic constants were determined from appropriate plots and equations as described in the Experimental section. The data represent the mean values obtained in two or three independent experiments.

$K_{mA}$ and $K_{mB}$, are the Michaelis Menten constants for A and B, and $K_I$ is the inhibition constant of product, P.

Although the kinetic results are presented in graphs of double reciprocal form, all data analyses were performed on a best fit to the hyperbolic form of rate equations using the iterative minimum $X^2$ nonlinear regression method of Leatherbarrow [42] to avoid errors inherent to linear plot estimations. Kinetic constants derived from the best fit results were then compared to the estimates calculated from the intercept and slope replots. All kinetic constants are reported as the mean determined from two to three independent experiments.

### *TPST-2 Covalent Intermediate*

TPST-2 (0.16 nmol) and 50 μM $^{35}$S-PAPS (50 μM) were incubated for 6 h at 37 °C in the presence or absence of recombinant human factor IX (0.4 nmol, BeneFIX; Wyeth Pharmaceuticals Inc., Philadelphia, PA, USA). Reactions were performed in 0.1 M NaCl, 20 mM 1,4-piperazinediethanesulfonic acid (PIPES), pH 6.9, 2 mM EDTA in a 100 μL final volume. Samples were then boiled in Laemmli SDS sample buffer and electrophoresed on 4%–15% Tri-glycine SDS polyacrylamide gels under non-reducing conditions and proteins stained with GelCode Blue (Thermo Fisher Scientific, Pittsburgh, PA, USA). The gels were dried and subjected to autoradiography using BioMax MS film (Kodak, Sigma-Aldrich, St. Louis, MO, USA). The bands were excised, dissolved in 30% $H_2O_2$ (60 °C, 15 h) and counted by liquid scintillation counting. Based on the counts, it was estimated that under these conditions 0.026 mol of sulfate were incorporated per mole of TPST-2.

### *Chemical Modification of TPST-2*

TPST-2 under non-reducing conditions was incubated with an excess of the respective reagent (DEPC, diethylpyrocarbonate at 10 mM; DTNB, 5′5-dithio-bis(2-nitrobenzoic acid) at 10 mM) for 10 min at pH 7.5, 30 °C. Both DTNB and DEPC in aqueous condition undergo hydrolysis which means it is not likely to interfere with the assay. TPST-2 assays were performed with 375 nM TPST-2, 500 μM nonsulfated CCR8, and 200 μM PAPS, and normalized by comparison with the activity of the unmodified enzyme as control. Experiments were repeated three times and results were averaged.

### *Multiple Sequence Alignment*

To identify conserved regions in TPST-2, 28 identified and predicted TPST-1 and -2 sequences from different species were retrieved from NCBI Protein database. All sequences with at least 40% sequence identity were analyzed by multiple sequence alignment generated using ClustalW [43]. The sequences were then further analyzed by aligning them with protein sequences of other well-studied sulfotransferases from different species: six NodH STs, 10 heparan sulfate 3-O-sulfotransferases (HS-3-OST), seven heparan sulfate 2-O-sulfotransferases (HS-2-OST), 10 heparan sulfate 6-O-sulfotransferases (HS-6-OST), three sulfotransferase domains of N-deacetylase/N-sulfotransferase (HS-N-ST), and four cytosolic STs including EST. The information gathered was then used to identify and compare the presence of conserved structural motifs of ST family in TPSTs. TPST and NodST sequences were also compared to distinguish if there is a similarity between TPSTs and the NodST tryptic peptide identified to contain the sulfuryl group of its covalent intermediate [17].

## Results

### *Initial Velocity Studies*

Two-substrate site kinetic studies of the forward reactions were performed using TPST-2 in the absence of added products for reactions using nonCCR8 and sY15CCR8 as acceptor substrates. Initial velocities were

measured in a matrix of varied concentrations of PAPS and CCR8 peptide substrates. Double reciprocal plots of $1/v$ versus 1/[S] at various fixed concentrations of the second substrate in Figure 2 indicate a set of parallel lines with the same slopes, which is indicative of a typical ping-pong mechanism.

Figure 2a shows the Lineweaver Burk plot for the sulfation of CCR8 at Y15 with nonCCR8 as the varied substrate and PAPS at different fixed concentrations. Repeated experiments and plots of the same data gave similar results with no reproducible trend toward curvature or intersection of the lines. Kinetic constants determined from fits of these primary data to eq 4 are listed in Table 1. Intercept replots from the primary data with respect to reciprocal concentrations of the fixed substrates were also linear as seen in Supporting Information 2, A–B. Based on the calculations from the replots, the estimated $V_{max}$ is 6.7 mU/mg protein (where 1 Unit (U) is equal to 1 $\mu$mol product formed per min), $K_{m,PAPS}$ is 8.4 $\mu$M, and $K_{m,nonCCR8}$ is 23.9 $\mu$M, which are all comparable to the values in Table 1 generated from fitting all data to eq 4. Specificity constants calculated from Table 1 values are as follows: $k_{cat}/K_m$ for nonCCR8 is $2.7 \times 10^2$ $M^{-1}s^{-1}$, $k_{cat}/K_m$ for PAPS is $5.9 \times 10^2$ $M^{-1}s^{-1}$. The turnover number, $k_{cat}$, for sulfation of nonCCR8 is $5.1 \times 10^{-3}$ mol of substrate converted to product per second.

We similarly performed the kinetic studies with sY15CCR8, a monosulfated CCR8 peptide, as substrate. Lineweaver-Burk plots in Figure 2b also show a series of parallel lines when either sY15CCR8 or PAPS is the varied substrate, which is fully consistent with a ping-pong mechanism. Consequently, intercept replots from the primary data with respect to reciprocal concentrations of the fixed substrates were also linear (Supporting Information 2, C–D) and the estimated kinetic constants ($V_{max}$ = 1.7 mU/mg protein, $K_{m,PAPS}$ = 3.7 $\mu$M, and $K_{m,sY15CCR8}$ = 2.6 $\mu$M) are all comparable to the corresponding values in Table 1. Specificity constants calculated from Table 1 values are as follows, $k_{cat}/K_m$ of sY15CCR8 is $4.3 \times 10^2$ $M^{-1}s^{-1}$, $k_{cat}/K_m$ of PAPS is $2.8 \times 10^2$ $M^{-1}s^{-1}$, with a $k_{cat}$ value of $1.3 \times 10^{-3}$ $s^{-1}$. As previously reported, the $K_m$ value for sY15CCR8 is lower than the nonsulfated CCR8. This indicates that binding is inherently tighter between sY15CCR8 and TPST-2, and that prior sulfation is likely to increase the efficiency of additional subsequent sulfation.

The duplication of pattern between the two reactions demonstrates that the series of parallel lines observed is indeed a reflection of a ping-pong catalytic mechanism for TPST-2 and not an artifact of the specific substrate.

## *Product Inhibition*

To distinguish between a classical one-site and a two-site ping-pong mechanism for TPST-2 bisubstrate system, initial velocities of the enzyme were measured in the presence of reaction by-product PAP for both Reaction 1, sulfation of nonCCR8 and Reaction 2, sulfation of sY15CCR8. For Reaction 2, PAP inhibited the reaction competitively with respect to PAPS as the varied substrate, and noncompetitively with respect to sY15CCR8 as the varied substrate as seen in Figure 3a and b. Secondary replots of slopes and y-intercepts with respect to PAP concentrations show that all inhibition patterns are linear functions. The corresponding calculated $K_I$ values for PAP from the replots are close to the constants determined by fitting the data to eqs 5 and 6 (Table 1): $K_{I,PAP}$ with respect to PAPS is 0.2 $\mu$M, and $K_{I,PAP}$ with respect to sY15CCR8 is 3.8 $\mu$M. These results were generated from two independent experiments. Similar PAP inhibition patterns were observed for Reaction 1 (data not shown).

## *Sulfated TPST-2 Intermediate*

To assess if a sulfated TPST-2 intermediate is formed during the catalytic cycle, three sulfation reactions were

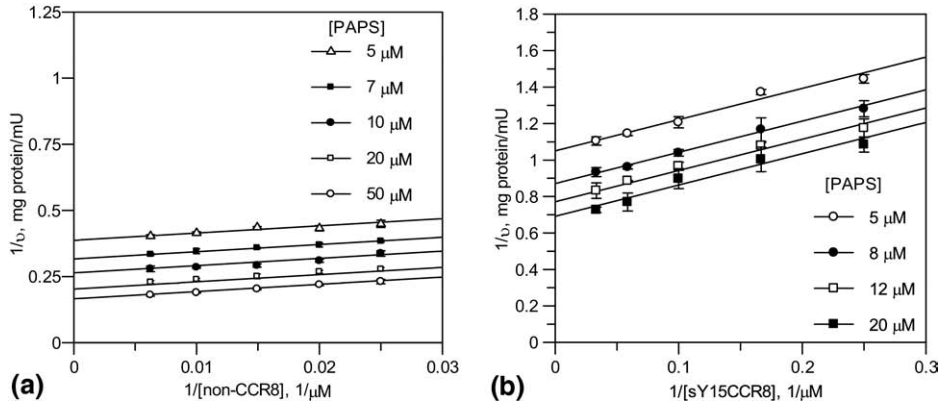


**Figure 2.** Initial velocity patterns for TPST-2 catalyzed sulfation of nonCCR8 and sulfation of sY15CCR8. $1/v$ values were plotted against (**a**) 1/[nonCCR8] at various fixed concentrations of PAPS; and (**b**) 1/[sY15CCR8] at various fixed concentrations of PAPS. Intercept replots of the primary plots can be found in the supporting information section. Data represent the mean ± standard deviation of three independent experiments.

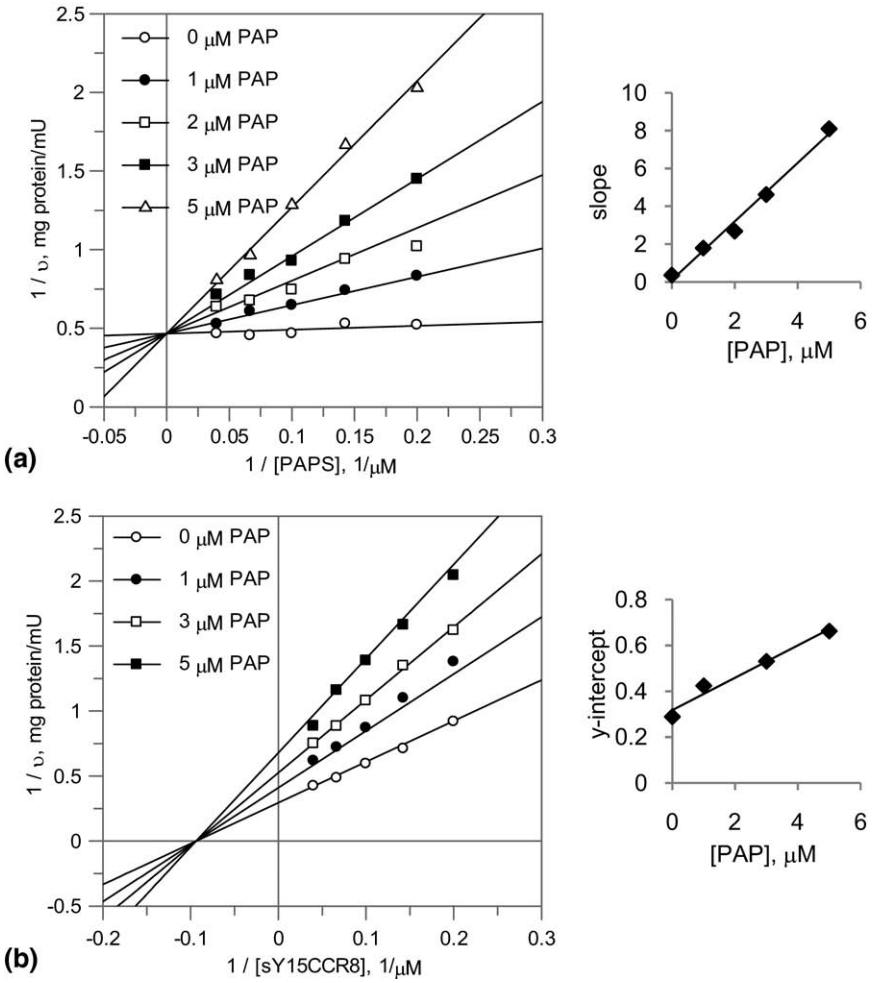


**Figure 3.** Inhibition patterns in the presence of PAP at pH 7.5, 30 °C. (**a**) $1/\upsilon$ versus 1/[PAPS] plots at 5, 7, 10, 15, and 25 $\mu$M [PAPS] and at different fixed concentrations of PAP while keeping [sY15CCR8] constant at 25 $\mu$M. Slope replot yields the equation $K_{I,slope} = (K_{m,B}/(V_{max}\,K_I))\,[I] + (K_{m,B}/V_{max})$ where the slope can be used to estimate $K_I$. (**b**) $1/\upsilon$ versus 1/[sY15CCR8] plots at 5,7,10,15 and 25 $\mu$M [sY15CCR8] and at different fixed concentrations of PAP while keeping [PAPS] constant at 25 $\mu$M. The intercept replot yields $K_{I,y\text{-}int} = 1/V_{max}\,([I]/K_I) + 1/V_{max}$. Data represent the mean of two independent experiments.

performed and acceptor products were separated by SDS-PAGE and analyzed by autoradiography. Figure 4 shows that when $^{35}$S-PAPS and factor IX were combined in the presence (lane 1) or absence of TPST-2 (lane 2), $^{35}$S-sulfuryl group transfer to factor IX occurred only in the presence TPST-2, demonstrating that sulfation was enzyme dependent. When $^{35}$S-PAPS and TPST-2 were combined in the absence of factor IX (lane 3) incorporation of $^{35}$S-sulfate into TPST-2 was observed demonstrating formation of a $^{35}SO_3$-TPST-2 covalent intermediate. However, the sulfated intermediate was not observed when factor IX was present (lane 1). These results indicate that a short-lived sulfated TPST-2 covalent intermediate is formed before the release of reaction products.

## *TPST-2 Chemical Modification*

At the reaction pH 7.5, only histidine and cysteine side chains are expected to be neutral and can be sulfurylated to form the TPST-2 covalent intermediate. Two chemical modifying agents, DEPC and DTNB, were incubated with TPST-2 individually before its reaction with substrates. Supporting information 3 shows that TPST-2 incubation with DEPC dramatically decreased TPST-2 activity to 4.4%, suggesting that one or more histidine residues are critically important for catalysis [44–46]. Whether a sulfohistidine covalent intermediate is formed or not is uncertain. In contrast, the activity of TPST-2 incubated with DTNB was comparable to that of the control indicating that cysteine residues do not participate in catalysis.

## *Multiple Sequence Alignment*

Twenty-eight TPST protein sequences (Supporting Information 4) were aligned with forty sequences of cytosolic, bacterial, and membrane-associated carbohydrate sulfotransferases to determine if the conserved 5′ PSB and 3′ PB structural motifs of ST family are present

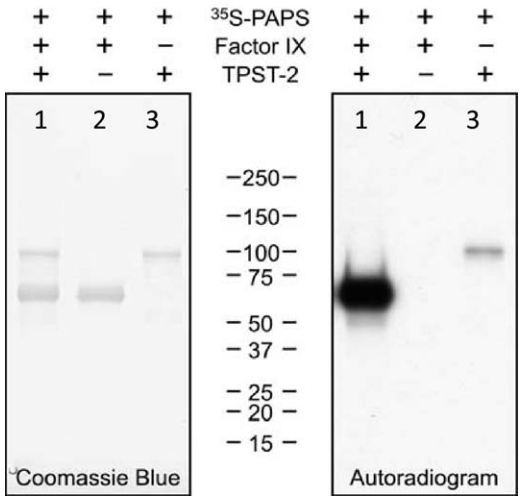


**Figure 4.** Detection of sulfated TPST-2 intermediate. $^{35}$S-PAPS and factor IX were combined in the presence (lane 1) or absence of TPST-2 (lane 2) or $^{35}$S-PAPS and TPST-2 were combined in the absence of factor IX (lane 3) for 6 h at 37 °C as described in Experimental Procedures. Samples were electrophoresed under non-reducing conditions and separated proteins stained with colloidal Coomassie (left panel). The same gel was then dried and subjected to autoradiography (right panel).

in TPST-2 (data not shown). As expected, the amino acid residues involved in the PAP/PAPS binding domain of STs are all highly conserved in TPSTs (Supporting Information 4, underlined and bold) [47–52]. These are amino acid residues Thr51, Thr52, Arg130, and Ser138 in mouse EST (Thr81, Thr82, Arg183, Ser191 in human TPST-2). In contrast, Lys48 of mEST corresponds to Arg78 for TPST-2 (Supporting Information 4, italicized and bold) and Arg18 of NodSTs even when Lys48 is highly conserved in all other 34 STs analyzed. Two other mEST amino acids involved in ST catalysis, Lys106 and His108, were also present in TPSTs (Lys147 and His148) and NodSTs (Lys76 and His79) (Supporting Information 4, bold).

Previous work by our group on the two-site ping pong catalytic mechanism of bacterial NodH ST detected the presence of a sulfated NodST intermediate by ESI-FT-ICR mass spectrometry [17]. The NodST tryptic peptide $T_{2-3}$ (T19GTHYLEELVNEHPNVLSNGELLNTYDTNWPDKER35) was identified to contain a sulfuryl group. Sequence alignment between TPSTs, NodSTs and the sulfurylated tryptic peptide shows clearly five highly conserved amino acids: Gly20, Thr21, His31, Pro32, and Gly38 (Supporting Information 5, underlined and bold). This suggests the possibility that a sulfurylated amino acid of TPST-2 exists in one of its corresponding amino acids.

## Discussion

The initial velocity double reciprocal plot patterns of the relationship between pairs of substrates obtained for both sulfation of nonCCR8 and sY15CCR8 by TPST-2 showed a series of parallel lines. These results suggest that the tyrosine sulfation reaction obeys the rate equation,

$$1/v = (K_{mA}/V_{max})\ 1/[A] + 1/V_{max}\ (1 + (K_{mB}/[B])) \qquad (7)$$

which is the linear function of the rate equation derived for a classical one-site ping-pong mechanism. This mode of catalysis requires the formation of a short-lived covalent enzyme intermediate which we identified upon the incubation of TPST-2 with the $^{35}$S-labeled sulfate donor in the absence of the sulfate acceptor (Figure 4). The TPST-2 covalent intermediate is formed between the release of the first product, PAP, and addition of the second substrate, sulfate acceptor peptide. The initial velocity data and the presence of $^{35}$S-sulfate labeled enzyme intermediate clearly precludes the possibility of a sequential catalytic mechanism for TPST-2; the latter involving binding of both substrates forming a ternary complex before sulfuryl group transfer followed by product release in a specific or random order. This mode of catalysis is reported to be the more common mechanism for well-studied cytosolic and bacterial sulfotransferases [11–14].

While the initial velocity data and the presence of $^{35}$S-sulfate labeled enzyme intermediate are consistent with a classical one-site ping-pong mechanism, the product inhibition patterns for both sulfation reactions are not. In the case of a classical ping-pong mechanism for sulfation of sY15CCR8, the substrate PAPS and disulfated product sY15sY17CCR8 would bind at a common site on the free enzyme form, TPST-2, and the substrate sY15CCR8 peptide and product PAP also combine at this same common site but with a modified enzyme form, TPST-2-$SO_3$, the substituted enzyme. As a consequence, product inhibition patterns between either PAPS and sY15sY17CCR8 or sY15CCR8 and PAP will be competitive at saturating concentrations of the nonvaried substrate. Conversely, product inhibition patterns obtained between either PAPS and PAP or sY15sY17CCR8 and sY15CCR8 peptides, which combine with different forms of the enzyme, will be noncompetitive. The results obtained with TPST-2 gave exactly opposite sets of PAP product inhibition patterns: PAP as a competitive inhibitor of PAPS (Figure 3a), while PAP as a noncompetitive inhibitor of monosulfated sY15CCR8 substrate (Figure 3b). The same PAP inhibition patterns were observed with respect to PAPS and nonsulfated CCR8 substrates (plots not shown). Taken together, these results are consistent with a two-site ping-pong mechanism where the substrates PAPS and sY15CCR8 peptide bind independently and randomly at two different binding sites separated physically on TPST-2 as opposed to the classical one-site model [41, 53, 54]. One site binds the peptides, and the other site binds to the adenosine coenzyme where sulfation and desulfation occurs at both sites. It is assumed that all substrates and products bind and dissociate independently in a rapid equilibrium ran-

dom fashion; that is, a peptide containing a tyrosine residue can combine at site one before or after PAPS binds at site two and the binding of one ligand has no effect on the binding of the other. Similarly, the presence of a substrate at one site does not influence the rate of sulfate transfer at the other site. Given that a sulfated TPST-2 intermediate is identified, the amino acid residue carrying the sulfuryl group is likely flexible enough to migrate between the two binding sites during the execution of its function as a sulfuryl-transferring agent. Therefore, as adapted from the two-site ping-pong model of transcarboxylase reported by Northrop [53], the forward reaction of TPST-2 tyrosine sulfation of nonsulfated CCR8 is summarized as follows: PAPS binds to its binding site and the sulfuryl group is transferred to the side-chain of an amino acid in TPST-2. Binding of the nonsulfated CCR8 and possible dissociation of PAP occurs randomly and independently. The flexible sulfated amino acid residue then migrates adjacent to the binding site of nonCCR8 and a second transfer reaction occurs to form the monosulfated CCR8 product. Finally, the sY15CCR8 product dissociates from the enzyme surface.

Through radioactive labeling experiments, we were able to establish the presence of a sulfated TPST-2 intermediate. A sulfated enzyme intermediate was reported previously in a bacterial sulfotransferase NodST, a two-site ping-pong enzyme, through in-solution digestion experiments and ESI/FT-ICR MS analysis [16, 17]. The sulfuryl moiety was identified to be present in the tryptic peptide $T_{2-3}$ (a.a. 19–53) of the NodST intermediate. Multiple sequence alignment of six NodSTs and the $T_{2-3}$ peptide together with twenty-eight TPSTs shows five highly conserved amino acids with Thr81 and His91 of human TPST-2 as possible candidates to be the sulfuryl-carrying nucleophilic amino acid (Supporting Information 5).

Earlier crystal structure studies on mouse EST showed similarities between kinases and sulfotransferases. In some phosphotransferase reactions, the phosphate group is transferred to a histidine residue to form a phosphohistidine intermediate before product formation [55]. Hence, it was proposed by Kakuta and coworkers that a histidine residue present in the catalytic site of STs may become sulfurylated to form a sulfohistidine intermediate before the sulfurylated product [47]. This is an alternative to the formation of a ternary complex identified to be present in sequential mechanism of several STs. We suggest that His91 is the possible sulfuryl moiety carrier in the TPST-2 intermediate with the conserved His148 as the catalytic base necessary to deprotonate the tyrosine-containing peptide substrate. His91 resides in a highly conserved region of TPSTs right next to the 5′PSB loop. This agrees with the possibility of His91 carrying the sulfuryl group and migrate between PAPS and peptide/protein binding sites. Supporting Information 6 shows a possible reaction mechanism of TPST for the substrates PAPS and tyrosine-containing protein. The proposed mechanism was recently reported by Malojcic and coworkers on aryl sulfotransferase (ASST), another ping-pong ST, from uropathogenic *E. coli* [45]. They proposed that upon the sulfation of His436 of ASST, the sulfuryl moiety of the sulfohistidine intermediate is stabilized by an extensive network of hydrogen bonding to the side chains of highly conserved two additional His, one each of Arg, Asn, and the N-backbone of Thr. This additional essential role of possible His residues in the catalytic site of TPSTs was further supported by the inactivation of TPST-2 through treatment with DEPC, a reagent that specifically modifies His side chains. Sequence alignment of 28 TPST homologs revealed more histidine residues to be invariant: His190, His244, His266, and His267. Two or more of these His residues may be involved in the hydrogen bonding network stabilizing the TPST sulfohistidine intermediate. Interestingly, it was reported that a mutation in the *Tpst2* gene is responsible for an autosomal recessive form of primary hypothyroidism in the growth-retarded *grt/grt* mouse [56]. The mutation (C798G) results in a H266Q substitution in TPST-2. In this report the authors showed that wild type TPST-2, but not wild type TPST-1 or the H266Q TPST-2 mutant, could sulfate a peptide modeled on a tyrosine sulfation site in the thyroid-stimulating hormone receptor (TSH-R) in vitro, suggesting that TPST-2, but not TPST-1, can efficiently sulfate TSH-R in vivo.

Because of indirect evidence showing the possible formation of a TPST-2 sulfohistidine intermediate, we performed in-solution digestion experiments on TPST-2 incubated with PAPS followed by MS analysis. TPST-2 with and without PAPS were digested with trypsin, chymotrypsin and/or glu-C endoproteinase. Three different mass spectrometers were used for analysis: Bruker ESI-FT-ICR MS in negative ionization mode, Thermo Electron LTQ-FT-ICR equipped with a nano-Acquitty UPLC system in positive mode, and LTQ-Orbitrap directly coupled to a Surveyor HPLC system in positive mode. Both hybrid instruments were programmed to perform MS3 experiments with neutral loss scan event for the loss of a sulfuryl group. All MS analyses had mass accuracy $< 10$ ppm with sequence coverages between 63% and 77%. All His containing peptides were identified to be present. Unfortunately, none of the experiments showed proof of a sulfuryl-carrying amino acid. It is likely due to a very low abundance intermediate and perhaps one that is quite unstable. As noted in the Experimental section, for every mole of TPST-2, only 0.026 mol is sulfated. New methodology will be required to enrich for the sulfated intermediate; unfortunately, we do not currently have such a method in place but one is now being planned.

Kinetic properties of TPST-2 sulfation reactions presented in Table 1 are consistent with our previous research which provided the apparent kinetic constants of TPST-2, TPST-1 and its mixture [39]. As expected, the $K_m$ value of nonsulfated CCR8 peptide is at least five times higher than the monosulfated peptide counter-

part, thus sY15CCR8 binds more tightly to TPST-2 compared to nonCCR8. However, the lower turnover number of the disulfation reaction indicates that TPST-2 catalyzes the monosulfation reaction four times more rapidly from substrate to product once the active sites are filled. To resolve this dichotomy and any effects of [S] with respect to $K_m$ in the reactions, $k_{cat}/K_m$ values are reported and indicate that sY15CCR8 is the more suitable substrate than nonCCR8 for TPST-2. Comparing the specificity constants of the respective substrates of the two sulfation reactions, PAPS is the preferred substrate over nonCCR8, while sY15CCR8 peptide becomes preferred than PAPS. These comparisons indicate that there are important interactions between the negative charges on the sulfate moiety of the sulfated peptide and the active sites of TPST-2.

TPST-2 specificity constants reported are relatively low compared to other values for sulfotransferases. It can be attributed to the fact that we used artificial substrates instead of the intact membrane-bound CC chemokine receptor 8 which is the true substrate in vivo. Much lower values for similar artificial substrates were published previously by another group which showed at least 10,000-fold lower specificity constants [37]. Another possible reason can be ascribed to the less conserved Lys48 residue of mEST in TPST-2. Interestingly, Lys48 is substituted by Arg78 at the 5′PSB motif of TPST-2. Arg is a more basic amino acid than Lys, hence the corresponding conjugate acid of Arg is less acidic than Lys. Therefore, Arg exhibits weaker hydrogen bonding interactions with the bridging oxygen between the 5′phosphate and sulfate groups of PAPS. This can slow down bond breaking between the two groups for the rest of the reaction to proceed, therefore affecting the $k_{cat}$ of the reaction. Furthermore, in a previously published study on mEST, a K48R mutation caused the $k_{cat}$ of the enzyme to drop at least 4-fold compared to wild type without changing the $K_m$ of the substrates [49].

In conclusion, initial rate kinetic analyses in the absence and presence of product PAP, and detection of a sulfated TPST-2 covalent intermediate via [$^{35}$S] radioactive labeling experiment were used to elucidate the catalytic mechanism of recombinant human TPST-2. Multiple sequence alignment of 68 sulfotransferases, including 28 TPSTs, together with chemical modification experiments, provided some insights on the location of the sulfuryl-carrying amino acid in the TPST-2 covalent intermediate. However, a more direct validation of the presence of a sulfohistidine intermediate will be required for future studies. Future studies are also necessary to elucidate the potential roles of other specific TPST-2 residues in the tyrosine sulfation mechanism.

Our analysis is consistent with a rapid equilibrium random two-site ping-pong mechanism for TPST-2. This is the first detailed study of the reaction kinetics and catalytic mechanism of a Golgi-resident sulfotransferase. Our research on the enzymatic properties and mode of catalysis of TPST-2 provides a platform for understanding the roles of membrane-associated STs in humans, particularly in tyrosine sulfation of chemokine receptors, and will aid in discovering potential drug inhibitors to this emerging novel class of therapeutic agents [8].

## Acknowledgments

The authors gratefully acknowledge funding for this research provided by grants from the National Institute of Health GM063581 (to J.A.L.) and HD056022 (to K.L.M. and J.A.L.). They thank Dr. Raluca Stefanescu and Dr. Richard Eigenheer for their technical assistance.

## Appendix A Supplementary Material

Supplementary material associated with this article may be found in the online version at doi:10.1016/j.jasms.2010.03.037.

## References

1. Farzan, M.; Mirzabekov, T.; Kolchinsky, P.; Wyatt, R.; Cayabyab, M.; Gerard, N. P.; Gerard, C.; Sodroski, J.; Choe, H. Tyrosine Sulfation of the Amino Terminus of CCR5 Facilitates HIV-1 Entry. *Cell* **1999,** *96,* 667–676.
2. Kehoe, J. W.; Bertozzi, C. R. Tyrosine sulfation: a modulator of extracellular protein-protein interactions. *Chem Biol.* **2000,** *7,* R57–61.
3. Bowman, K. G.; Bertozzi, C. R. Carbohydrate Sulfotransferases: Mediators of Extracellular Communication. *Chem. Biol.* **1999,** *6,* R9–R22.
4. Habuchi, O. Diversity and Functions of Glycosaminoglycan Sulfotransferases. *Biochim. Biophys. Acta* **2000,** *1474,* 115–127.
5. Falany, C. N. Enzymology of Human Cytosolic Sulfotransferases. *FASEB J.* **1997,** *11,* 206–216.
6. Falany, C. N. Sulfation and Sulfotransferases. Introduction: Changing View of Sulfation and the Cytosolic Sulfotransferases. *FASEB J.* **1997,** *11,* 1–2.
7. Gamage, N.; Barnett, A.; Hempel, N.; Duggleby, R. G.; Windmill, K. F.; Martin, J. L.; McManus, M. E. Human Sulfotransferases and Their Role in Chemical Metabolism. *Toxicol. Sci.* **2006,** *90,* 5–22.
8. Armstrong, J. I.; Bertozzi, C. R. Sulfotransferases as Targets for Therapeutic Intervention. *Curr. Opin. Drug Discov. Dev.* **2000,** *3,* 502–515.
9. Whittemore, R. M.; Pearce, L. B.; Roth, J. A. Purification and Kinetic Characterization of a Dopamine-Sulfating Form of Phenol Sulfotransferase from Human Brain. *Biochemistry* **1985,** *24,* 2477–2482.
10. Whittemore, R. M.; Pearce, L. B.; Roth, J. A. Purification and Kinetic Characterization of a Phenol-Sulfating Form of Phenol Sulfotransferase from Human Brain. *Arch. Biochem. Biophys.* **1986,** *249,* 464–471.
11. Varin, L.; Ibrahim, R. K. Novel Flavonol 3-Sulfotransferase. Purification, Kinetic Properties, and Partial Amino Acid Sequence. *J. Biol. Chem.* **1992,** *267,* 1858–1863.
12. Zhang, H.; Varlamova, O.; Vargas, F. M.; Falany, C. N.; Leyh, T. S. Sulfuryl Transfer: The Catalytic Mechanism of Human Estrogen Sulfotransferase. *J. Biol Chem.* **1998,** *273,* 10888–10892.
13. Vakiani, E.; Luz, J. G.; Buck, J. Substrate Specificity and Kinetic Mechanism of the Insect Sulfotransferase, Retinol Dehydratase. *J. Biol. Chem.* **1998,** *273,* 35381–35387.
14. Pi, N.; Hoang, M. B.; Gao, H.; Mougous, J. D.; Bertozzi, C. R.; Leary, J. A. Kinetic Measurements and Mechanism Determination of Stf0 Sulfotransferase Using Mass Spectrometry. *Anal. Biochem.* **2005,** *341,* 94–104.
15. Kwon, A. R.; Yun, H. J.; Choi, E. C. Kinetic Mechanism and Identification of the Active Site Tyrosine Residue in *Enterobacter amnigenus* Arylsulfate Sulfotransferase. *Biochem. Biophys. Res. Commun.* **2001,** *285,* 526–529.
16. Pi, N.; Armstrong, J. I.; Bertozzi, C. R.; Leary, J. A. Kinetic Analysis of NodST Sulfotransferase Using an Electrospray Ionization Mass Spectrometry Assay. *Biochemistry* **2002,** *41,* 13283–13288.
17. Pi, N.; Yu, Y.; Mougous, J. D.; Leary, J. A. Observation of a Hybrid Random Ping-Pong Mechanism of Catalysis for NodST: A Mass Spectrometry Approach. *Protein Sci.* **2004,** *13,* 903–912.
18. Preobrazhensky, A. A.; Dragan, S.; Kawano, T.; Gavrilin, M. A.; Gulina, I. V.; Chakravarty, L.; Kolattukudy, P. E. Monocyte Chemotactic Protein-1 Receptor CCR2B is a Glycoprotein that has Tyrosine Sulfation in a Conserved Extracellular N-Terminal Region. *J. Immunol.* **2000,** *165,* 5295–5303.

19. Gutierrez, J.; Kremer, L.; Zaballos, A.; Goya, I.; Martinez, A. C.; Marquez, G. Analysis of Post-Translational CCR8 Modifications and Their Influence on Receptor Activity. *J. Biol. Chem.* **2004,** *279,* 14726–14733.
20. Colvin, R. A.; Campanella, G. S.; Manice, L. A.; Luster, A. D. CXCR3 Requires Tyrosine Sulfation for Ligand Binding and a Second Extracellular Loop Arginine Residue for Ligand-Induced Chemotaxis. *Mol. Cell. Biol.* **2006,** *26,* 5838–5849.
21. Farzan, M.; Babcock, G. J.; Vasilieva, N.; Wright, P. L.; Kiprilov, E.; Mirzabekov, T.; Choe, H. The Role of Post-Translational Modifications of the CXCR4 Amino Terminus in Stromal-Derived Factor 1 $\alpha$ Association and HIV-1 Entry. *J. Biol. Chem.* **2002,** *277,* 29484–29489.
22. Seibert, C.; Veldkamp, C. T.; Peterson, F. C.; Chait, B. T.; Volkman, B. F.; Sakmar, T. P. Sequential Tyrosine Sulfation of CXCR4 by Tyrosylprotein Sulfotransferases. *Biochemistry* **2008,** *47,* 11251–11262.
23. Fong, A. M.; Alam, S. M.; Imai, T.; Haribabu, B.; Patel, D. D. CX. 3CR1 Tyrosine Sulfation Enhances Fractalkine-Induced Cell Adhesion. *J. Biol. Chem.* **2002,** *277,* 19418–19423.
24. Moon, A. F.; Edavettal, S. C.; Krahn, J. M.; Munoz, E. M.; Negishi, M.; Linhardt, R. J.; Liu, J.; Pedersen, L. C. Structural Analysis of the Sulfotransferase (3-o-Sulfotransferase Isoform 3) Involved in the Biosynthesis of an Entry Receptor for Herpes Simplex Virus 1. *J. Biol. Chem.* **2004,** *279,* 45185–45193.
25. Edavettal, S. C.; Lee, K. A.; Negishi, M.; Linhardt, R. J.; Liu, J.; Pedersen, L. C. Crystal Structure and Mutational Analysis of Heparan Sulfate 3-O-Sulfotransferase Isoform 1. *J. Biol. Chem.* **2004,** *279,* 25789–25797.
26. Munoz, E.; Xu, D.; Kemp, M.; Zhang, F.; Liu, J.; Linhardt, R. J. Affinity, Kinetic, and Structural Study of the Interaction of 3-O-Sulfotransferase Isoform 1 with Heparan Sulfate. *Biochemistry* **2006,** *45,* 5122–5128.
27. Myette, J. R.; Shriver, Z.; Liu, J.; Venkataraman, G.; Rosenberg, R.; Sasisekharan, R. Expression in *Escherichia coli*, Purification and Kinetic Characterization of Human Heparan Sulfate 3-O-Sulfotransferase-1. *Biochem. Biophys. Res. Commun.* **2002,** *290,* 1206–1213.
28. Ouyang, Y. B.; Moore, K. L. Molecular Cloning and Expression of Human and Mouse Tyrosylprotein Sulfotransferase-2 and a Tyrosylprotein Sulfotransferase Homologue in *Caenorhabditis elegans*. *J. Biol. Chem.* **1998,** *273,* 24770–24774.
29. Ouyang, Y.; Lane, W. S.; Moore, K. L. Tyrosylprotein Sulfotransferase: Purification and Molecular Cloning of an Enzyme that Catalyzes Tyrosine O-Sulfation, a Common Post-Translational Modification of Eukaryotic Proteins. *Proc. Natl. Acad. Sci. U.S.A.* **1998,** *95,* 2896–2901.
30. Beisswanger, R.; Corbeil, D.; Vannier, C.; Thiele, C.; Dohrmann, U.; Kellner, R.; Ashman, K.; Niehrs, C.; Huttner, W. B. Existence of Distinct Tyrosylprotein Sulfotransferase Genes: Molecular Characterization of Tyrosylprotein Sulfotransferase-2. *Proc. Natl. Acad. Sci. U.S.A.* **1998,** *95,* 11134–11139.
31. Moore, K. L. The Biology and Enzymology of Protein Tyrosine O-Sulfation. *J. Biol. Chem.* **2003,** *278,* 24243–24246.
32. Hille, A.; Huttner, W. B. Occurrence of Tyrosine Sulfate in Proteins—a Balance Sheet. 2. Membrane Proteins. *Eur. J. Biochem.* **1990,** *188,* 587–596.
33. Hille, A.; Braulke, T.; von Figura, K.; Huttner, W. B. Occurrence of Tyrosine Sulfate in Proteins—a Balance Sheet. 1. Secretory and Lysosomal Proteins. *Eur. J. Biochem.* **1990,** *188,* 577–586.
34. Baeuerle, P. A.; Huttner, W. B. Tyrosine Sulfation of Yolk Proteins 1, 2, and 3 in *Drosophila melanogaster*. *J. Biol. Chem.* **1985,** *260,* 6434–6439.
35. Lee, R. W.; Huttner, W. B. (Glu62, Ala30, Tyr8)n Serves as High-Affinity Substrate for Tyrosylprotein Sulfotransferase: A Golgi Enzyme. *Proc. Natl. Acad. Sci. U.S.A.* **1985,** *82,* 6143–6147.
36. Niehrs, C.; Kraft, M.; Lee, R. W.; Huttner, W. B. Analysis of the Substrate Specificity of Tyrosylprotein Sulfotransferase Using Synthetic Peptides. *J. Biol. Chem.* **1990,** *265,* 8525–8532.
37. Mishiro, E.; Sakakibara, Y.; Liu, M. C.; Suiko, M. Differential Enzymatic Characteristics and Tissue-Specific Expression of Human TPST-1 and TPST-2. *J. Biochem. (Tokyo).* **2006,** *140,* 731–737.
38. Niehrs, C.; Huttner, W. B. Purification and Characterization of Tyrosylprotein Sulfotransferase. *EMBO J.* **1990,** *9,* 35–42.
39. Danan, L. M.; Yu, Z.; Hoffhines, A. J.; Moore, K. L.; Leary, J. A. Mass Spectrometric Kinetic Analysis of Human Tyrosylprotein Sulfotransferase-1 and -2. *J. Am. Soc. Mass Spectrom.* **2008,** *19,* 1459–1466.
40. MacRae, I.; Segel, I. H. ATP Sulfurylase from Filamentous Fungi: Which Sulfonucleotide is the True Allosteric Effector? *Arch. Biochem. Biophys.* **1997,** *337,* 17–26.
41. Segel, I. H. *Enzyme Kinetics: Behavior and Analysis of Rapid Equilibrium and Steady-State Enzyme Systems*; Wiley Classics Library ed.; Wiley: New York, 1993; p. xxii, p. 957.
42. Leatherbarrow, R. J. Use of Nonlinear Regression to Analyze Enzyme Kinetic Data: Application to Situations of Substrate Contamination and Background Subtraction. *Anal. Biochem.* **1990,** *184,* 274–278.
43. Chenna, R.; Sugawara, H.; Koike, T.; Lopez, R.; Gibson, T. J.; Higgins, D. G.; Thompson, J. D. Multiple Sequence Alignment with the Clustal Series of Programs. *Nucleic Acids Res.* **2003,** *31,* 3497–3500.
44. Chen, G. Histidine Residues in Human Phenol Sulfotransferases. *Biochem. Pharmacol.* **2004,** *67,* 1355–1361.
45. Malojcic, G.; Owen, R. L.; Grimshaw, J. P.; Brozzo, M. S.; Dreher-Teo, H.; Glockshuber, R. A Structural and Biochemical Basis for PAPS-Independent Sulfuryl Transfer by Aryl Sulfotransferase from Uropathogenic *Escherichia coli*. *Proc. Natl. Acad. Sci. U.S.A.* **2008,** *105,* 19217–19222.
46. Miles, E. W. Modification of Histidyl Residues in Proteins by Diethylpyrocarbonate. *Methods Enzymol.* **1977,** *47,* 431–442.
47. Kakuta, Y.; Pedersen, L. G.; Carter, C. W.; Negishi, M.; Pedersen, L. C. Crystal Structure of Estrogen Sulphotransferase. *Nat. Struct. Biol.* **1997,** *4,* 904–908.
48. Kakuta, Y.; Pedersen, L. G.; Pedersen, L. C.; Negishi, M. Conserved Structural Motifs in the Sulfotransferase Family. *Trends Biochem. Sci.* **1998,** *23,* 129–130.
49. Kakuta, Y.; Petrotchenko, E. V.; Pedersen, L. C.; Negishi, M. The Sulfuryl Transfer Mechanism. Crystal Structure of a Vanadate Complex of Estrogen Sulfotransferase and Mutational Analysis. *J. Biol. Chem.* **1998,** *273,* 27325–27330.
50. Pedersen, L. C.; Petrotchenko, E.; Shevtsov, S.; Negishi, M. Crystal Structure of the Human Estrogen Sulfotransferase-PAPS Complex: Evidence for Catalytic Role of Ser137 in the Sulfuryl Transfer Reaction. *J. Biol. Chem.* **2002,** *277,* 17928–17932.
51. Teramoto, T.; Sakakibara, Y.; Liu, M. C.; Suiko, M.; Kimura, M.; Kakuta, Y. Snapshot of a Michaelis Complex in a Sulfuryl Transfer Reaction: Crystal Structure of a Mouse Sulfotransferase, mSULT1D1, Complexed with Donor Substrate and Accepter Substrate. *Biochem. Biophys. Res. Commun.* **2009,** *383,* 83–87.
52. Sueyoshi, T.; Kakuta, Y.; Pedersen, L. C.; Wall, F. E.; Pedersen, L. G.; Negishi, M. A role of Lys614 in the Sulfotransferase Activity of Human Heparan Sulfate N-Deacetylase/N-Sulfotransferase. *FEBS Lett.* **1998,** *433,* 211–214.
53. Northrop, D. B. Transcarboxylase. VI. Kinetic Analysis of the Reaction Mechanism. *J. Biol. Chem.* **1969,** *244,* 5808–5819.
54. Wong, L. J.; Wong, S. S. Kinetic Mechanism of the Reaction Catalyzed by Nuclear Histone Acetyltransferase from Calf Thymus. *Biochemistry* **1983,** *22,* 4637–4641.
55. Wolodko, W. T.; Fraser, M. E.; James, M. N.; Bridger, W. A. The Crystal Structure of Succinyl-CoA Synthetase from *Escherichia coli* at 2.5-A Resolution. *J. Biol. Chem.* **1994,** *269,* 10883–10890.
56. Sasaki, N.; Hosoda, Y.; Nagata, A.; Ding, M.; Cheng, J. M.; Miyamoto, T.; Okano, S.; Asano, A.; Miyoshi, I.; Agui, T. A Mutation in Tpst2 Encoding Tyrosylprotein Sulfotransferase Causes Dwarfism Associated with Hypothyroidism. *Mol. Endocrinol.* **2007,** *21,* 1713–1721.